Oxygen Barrier Properties of PET Copolymers Containing Bis(2-Hydroxyethyl)hydroquinones

Genara S. Andrade,[1] David M. Collard,[1] David A. Schiraldi,[2] Yushan Hu,[3] Eric Baer,[3] Anne Hiltner[3]

[1]*School of Chemistry and Biochemistry and the Polymer Education and Research Center, Georgia Institute of Technology, Atlanta, Georgia 30332-0400*
[2]*KoSa, P.O. Box 5750, Spartanburg, South Carolina 29304-5750*
[3]*Department of Macromolecular Science and Center for Applied Polymer Research, Case Western Reserve University, Cleveland, Ohio 44106-7202*

Received 19 August 2002; accepted 20 September 2002

ABSTRACT: A series of poly[ethylene-*co*-bis(2-ethoxy)hydroquinone terephthalate], PET-*co*-BEHQ copolymers were prepared by polymerization of various substituted bis(2-hydroxyethyl)hydroquinones (BEHQs), dimethyl terephthalate (DMT), and ethylene glycol (EG). In addition to copolymers containing 6–16.5 mol % BEHQ, the homopolymer of BEHQ with dimethyl terephthalate, p(BEHQ-T), was also prepared. The thermal and barrier properties of amorphous materials were studied. As the amount of comonomer was increased, the T_g and T_m of the materials decreased relative to those of PET. Oxygen permeability also decreased with increasing comonomer content. This improvement in barrier-to-oxygen permeability was primarily due to a decrease in solubility of oxygen in the polymer. All of the copolymers tested displayed similar oxygen diffusion coefficients. The decrease in solubility correlates with the decrease in T_g.
 J Appl Polym Sci 89: 934–942, 2003

Key words: polyesters; barrier; diffusion

INTRODUCTION

There is great interest in the development of polymers with high barrier to oxygen permeation for use in the food packaging industry. Although poly(ethylene terephthalate) (PET) has good gas-barrier properties leading to its extensive use in packaging, its properties are not sufficient for the protection of highly oxygen-sensitive materials.[1] Oxygen permeation (*P*) through a polymer matrix is the product of gas solubility coefficient (*S*) and gas diffusion coefficient (*D*). Both diffusion and solubility are functions of free volume.[2] Decreasing the magnitude of either or both of these factors will improve the barrier that the polymer presents to penentrant molecules. This may be achieved either passively or actively. An active barrier decreases gas permeation through specific interactions or reactions of the gas permeant with the polymer itself. The recent advent of enhanced multilayer packaging materials based on PET makes use of layers of polymers that scavenge oxygen, such as poly(butadiene)[3] and polyamides.[4,5] A passive barrier has no such specific interaction between the penetrant molecules and the polymer matrix. Coating[6,7] or blending[8,9] a barrier polymer with another material that presents a higher barrier to oxygen is a common way to accomplish this. Most recently, there has been interest in the uniform incorporation of nanoclays[5] into barrier polymers. However, the development of high-performance, cost-efficient single-layer containers remains elusive. Another approach to the development of high-barrier materials is to prepare comonomers with structural units designed to change the passive[10,11] or active[3] barrier of PET.

A number of approaches have been developed to modify interchain packing in the amorphous phase of semicrystalline PET. These include incorporation of hydrogen-bonding structural units,[12] fused arenes,[10] and mesogens.[13] Incorporating units that introduce specific interactions between polymer chains improves interchain packing. For example, liquid crystalline polymers prepared from 4,4′-biphenol and 1,4-dialkylesters of pyromellitic acid form highly ordered crystals and mesophases. The electron-deficient rings of the pyromellitic tetraester in the polymer and the electron-rich bisphenol-derived structural units form interchain charge transfer complexes.[14] However, PET has only electron-deficient terephthalate aromatic rings. To explore the possibility of interchain interactions between electron-rich and electron-poor repeat units, we sought to incorporate electron-rich arenes into PET copolyesters. This article focuses on the in-

Correspondence to: D. M. Collard.
Contract grant sponsors: KoSa, UNCF-Merck Science Initiative, GEM Consortium.

Journal of Applied Polymer Science, Vol. 89, 934–942 (2003)

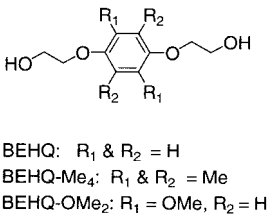

Figure 1 Structure of BEHQs.

corporation of bis(2-hydroxyethyl)hydroquinone (BEHQ), tetramethyl-bis(2-hydroxyethyl)hydroquinone (BEHQ-Me_4), and 2,5-dimethoxy-bis(2-hydroxyethyl)hydroquinone [BEHQ-$(OMe)_2$] into PET (Fig. 1). The hydroquinone group in BEHQ offers an electron-rich aromatic unit. Substituting BEHQ with electron-donating units such as methyl or methoxy groups serves to increase the electron density of the aromatic ring. This diol comonomer replaces ethylene glycol (EG) in the polymerization. If all the EG in PET is replaced with BEHQ, a homopolymer, p(BEHQ-T), is formed which has alternating electron-rich and electron-poor units (Fig. 2). Because of its high volatility and low reactivity (i.e., low nucleophilicity relative to EG), hydroquinone itself is difficult to incorporate into PET and the resulting aryl esters are less electron-rich than the aryl ethers of BEHQ. Hydroxyethylated hydroquinone, BEHQ, suffers from neither of these limitations. It is less volatile and the reactivity of this diol during polymerization is similar to that of EG.

Increased interchain interaction in the PET copolymers due to the formation of charge transfer complexes between hydroquinone and terephthalate units would cause a reduction in the free volume of the polymer leading to a decrease in O_2 permeation. Specific interactions between the polymer and molecular oxygen might also serve as a mechanism to decrease permeability. Oxygen forms weak complexes with electron-rich arenes.[15–17] This is evident from a red-shift in the onset of the ultraviolet visibility (UV–Vis) absorbance band of arenes in the presence of oxygen[18,19] and recent ^{13}C-cross polarization/magic angle spinning (CPMAS) T_1 experiments used to investigate interactions between oxygen and several arene-containing polymers.[20]

The copolymerization of BEHQs with PET introduces electron-rich arenes, which may interact with either electron-poor arenes or oxygen to improve the barrier properties of the polymer. Here we report the thermal and barrier properties of a series of amorphous PET-*co*-BEHQ copolymers containing various amounts of BEHQ, BEHQ-Me_4, and BEHQ-$(OMe)_2$, as well as the p(BEHQ-T) homopolymer. Although preliminary reports of the incorporation of BEHQ into PET[21] and PEN[22] have been made, there has been no discussion of the barrier properties of these materials.

EXPERIMENTAL

Materials, synthetic methods, and characterization

Commercial-grade dimethyl terephthalate (DMT) and EG for the preparation of PET copolymers were obtained from KoSa (Spartanburg, SC). All other reagents were purchased from Aldrich Chemical Co. (Milwaukee, WI) and used without further purification. Mass spectrums were obtained by using a VG 70SE mass spectrometer and a HP 5890 gas chromatogram. ^{1}H- and ^{13}C-NMR spectra were recorded on a Varian Gemini spectrometer at 300 and 75 MHz, respectively. The comonomer content of each polymer was determined by ^{1}H-NMR analysis. The polymer samples were dissolved in $CDCl_3$ containing 5% (v/v) trifluoroacetic acid (TFA-*d*). Thermal characteristics were determined by DSC analysis over a temperature range of 0 to 280°C with a heating rate of 10°C/min. Differential scanning calorimetry (DSC) was performed under nitrogen by using a Perkin–Elmer Series 7 differential scanning calorimeter. Molecular weights of the PET copolymers were determined by measurement of intrinsic viscosity (IV) using the formula, $M_n = 34{,}860(\mathrm{IV})^{1.205}$. Dilute solution viscometry was performed on an AVS 500 instrument at 25°C by using a 1% polymer solution in dichloroacetic acid.

Monomer synthesis

Durohydroquinone

Tin (II) chloride (27.7 g, 0.146 mol) was dissolved in concentrated hydrochloric acid (140 mL) and the so-

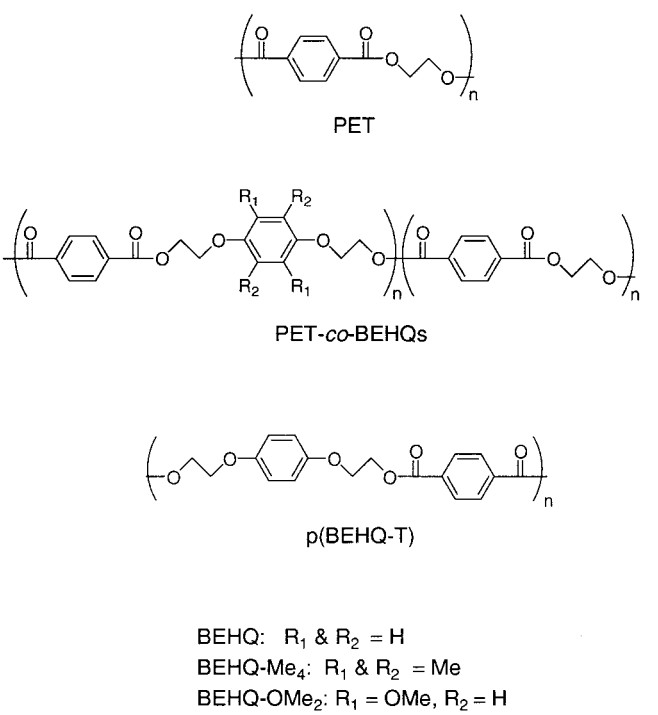

Figure 2 Structure of PET, PET-*co*-BEHQs, and p(BEHQ-T).

lution was diluted with water (280 mL). Duroquinone (26.6 g, 0.162 mol) was added to the solution and the mixture was stirred at 60°C for 12 h. The mixture was cooled, filtered, and washed with water (100 mL). The solid was recrystallized from ethanol to afford durohydroquinone as a peach solid (20.24 g, 75% yield).

Melting point (mp) 173°C (dec.). Lit. mp 171°C (dec.). ^{1}H-NMR (DMSO-d_6) δ2.03 (s, 12H). IR (cm^{-1}): 3390, 2927, 1315, 1233, 1061, 825, 606.

2,3,5,6-Tetramethyl-bis(2-hydroxyethyl)hydroquinone

Durohydroquinone (20.2 g, 0.122 mol), ethylene carbonate (22.5 g, 0.256 mol), and potassium iodide (1.00 g, 0.010 mol) were charged into a round-bottom flask with a mechanical stirrer and placed under nitrogen. The mixture was heated slowly to 200°C and held at this temperature until the reactants melted. The temperature was lowered to 170°C and the solution was stirred for 12 h. The solution was cooled to room temperature, dissolved in chloroform, and washed with 1% aqueous sodium hydroxide (2 × 200 mL). The solution was washed with water (1 × 200 mL) and the solvent was removed under reduced pressure. The resulting solid was stirred in hot hexane (350 mL) for 1 h. The mixture was filtered and the product was recrystallized from toluene to provide 2,3,5,6-tetramethyl-bis(2-hydroxyethyl)hydroquinone as an off-white solid (17.5 g, 57% yield).

mp 162°C. Lit. mp 163°C. ^{1}H-NMR (DMSO-d_6) δ3.67 (t, 4H), 3.60 (t, 4H), 2.09 (s, 12H). ^{13}C-NMR (DMSO-d_6) δ151.1, 127.2, 74.3, 60.3, 12.6. IR (cm^{-1}): 3368, 2927, 2874, 2368, 1657, 1558, 1255, 1077. MS (*m/z*): 254, 210, 165, 151, 137, 121, 105, 91.

2,5-Dimethoxyhydroquinone

1,4-Dimethoxybenzene (117 g, 0.850 mol) was dissolved in glacial acetic acid (1.59 L). Concentrated H_2SO_4 (4.5 mL) was added to the solution, followed by 30% H_2O_2 (1.29 L). After 24 h, yellow crystals appeared and the solution was allowed to sit until no more precipitate formed. The mixture was filtered and the crystals were washed with water (2 × 220 mL). The resulting solid was added to a solution of tin (II) chloride (66.0 g, 0.350 mol) in 4*M* HCl (648 mL). The mixture was stirred at 60°C for 12 h, cooled, filtered, and washed with water (300 mL). The product was recrystallized from ethanol to afford 2,5-dimethoxyhydroquinone as a white solid (42.37 g, 29% yield).

mp 236°C (dec.). Lit. mp 232°C. ^{1}H-NMR (DMSO-d_6) δ3.84 (s, 6H), 6.65 (s, 2H). IR (cm^{-1}): 3395, 1558, 1523, 1350, 1195, 1171, 861, 826.

2,5-Dimethoxy-bis(2-hydroxyethyl)hydroquinone

2,5-Dimethoxyhydroquinone (59.8 g, 0.350 mol) and ethylene carbonate (61.9 g, 0.700 mol) were dissolved in dimethylformamide (DMF; 655 mL). Sodium hydride (1.0 g, 0.040 mol) was added. The mixture was heated at 120°C for 36 h. The DMF was removed by distillation under reduced pressure and the residue was heated at 60°C under vacuum for 48 h to remove residual solvent. The crude product was extracted with benzene in a Soxhlet extractor. The benzene solution was cooled and filtered. The solid was recrystallized from toluene to afford 2,5-dimethoxy-bis(2-hydroxyethyl)hydroquinone as a white solid (37.93 g, 42% yield).

mp 129°C. ^{1}H-NMR (DMSO-d_6) δ6.69 (s, 2H), 4.79 (t, 2H), 3.92 (t, 4H), 3.66 (t, 4H), 3.70 (s, 6H). ^{13}C-NMR (DMSO-d_6) δ143.2, 142.2, 103.2, 71.5, 59.8, 56.6. IR (cm^{-1}): 3460, 3342, 2934, 1525, 1229, 1202, 1031, 1077. MS (*m/z*): 258, 226, 214, 169.

Copolymer preparation

PET copolymers containing various amounts of BEHQ (5, 10, 15, and 20%) and 10% BEHQ-Me_4 and 10% BEHQ-$(OMe)_2$ were prepared by a standard procedure for two-step polyesterification. The amount of BEHQ added was based on the amount of DMT charged in the reactor. The procedure for the preparation of the 10% PET-*co*-BEHQ copolymer is provided below.

DMT (243 g, 1.25 mol), EG (175 g, 2.80 mol), and manganese acetate (89 mg, 0.51 mmol) were charged into a stirred stainless steel reactor. The reactor was purged with N_2 and heated to 200°C. The reactor was held at 200°C for 20 min and the temperature was raised to 245°C and held for 45 min. Polyphosphoric acid (0.54 g of a 10% solution in EG), bis(2-hydroxyethyl)hydroquinone (24.8 g, 0.125 mol), and antimony trioxide (91 mg, 3.1 mol) were added. The reactor was heated to 285°C and repurged with N_2. The mixture was stirred for 20 min, and the pressure was lowered to 0.15 Pa over 1.5 h. The reactor was held at 285°C and 0.15 Pa for an additional 1.5 h. The reactor was then flushed with N_2. The polymer was removed from the reactor, quenched in cold water, and cryoground into small pellets.

PET-*co*-BEHQ: ^{1}H-NMR (19 : 1 $CDCl_3$/TFA-*d*) δ4.30 (bs, 4H, ArO—CH_2—), 4.73 (s, 4H, $ArCO_2$—CH_2—), 6.89 (s, 4H, —O—C_6H_4—O—), 8.10 (s, 4H, —O_2C—C_6H_4—CO_2—).

PET-*co*-BEHQ-Me_4: ^{1}H-NMR (19 : 1 $CDCl_3$/TFA-*d*) δ2.19 (s, 12H, O—Ar—CH_3), 4.10 (bs, 4H, ArO—CH_2—), 4.73 (s, 4H, $ArCO_2$—CH_2—), 8.11 (s, 4H, —O_2C—C_6H_4—CO_2—).

PET-*co*-BEHQ-$(OMe)_2$: ^{1}H-NMR (19 : 1 $CDCl_3$/TFA-*d*) δ3.79 (s, 6H, O—Ar—OCH_3), 4.38 (bs, 4H, ArO—CH_2—), 4.74 (s, 4H, $ArCO_2$—CH_2—), 6.70 (s, 2H, —O—C_6H_4—O—), 8.11 (s, 4H, —O_2C—C_6H_4—CO_2—).

Homopolymer preparation: p(BEHQ-T)

DMT (90.5 g, 0.467 mol), bis(2-hydroxyethyl)hydroquinone (92.0 g, 0.465 mol), zinc acetate (33.7 mg, 0.180

mmol), and antimony trioxide (0.124 g, 0.420 mmol) were combined in a stirred glass reactor under a N_2 atmosphere. The reactor was placed into an oil bath at 225°C. The reagents melted and the reactor was held at 225°C for 1 h. The temperature of the oil bath was raised to 250°C and held for 1 h and then raised to 280°C and held at that temperature for another hour. Vacuum was applied and the pressure was lowered to 0.05 Pa over 30 min. The polymerization was held at 280°C and 0.05 Pa for 2 h. The reactor was then flushed with N_2 and removed from the oil bath. The polymer was removed as the reactor cooled and was cryo-ground in small pieces. The resulting material was solid state polymerized by heating under N_2 at 200°C for 24 h.

^{1}H-NMR (19 : 1 $CDCl_3$/TFA-*d*) δ4.41 (bs, 4H, ArO—CH_2—), 4.76 (bs, 4H, $ArCO_2$—CH_2—), 6.98 (s, 4H, —O—C_6H_4—O—), 8.15 (s, 4H, —O_2C—C_6H_4—CO_2—).

Film preparation and characterization

The polymer pellets were dried under vacuum at 80°C for 24 h prior to molding. The dry pellets were compression molded and quenched into amorphous films as described previously.[23] The temperature of the press was 265°C for all of the materials. The amorphous films were stretched under constrained uniaxial conditions as described previously.[24] The film width before stretching was 130 mm; the thickness and gauge length were varied to achieve 100–200 μm. Grids were marked on the specimen to measure the draw ratio. The film was clamped between wide grips and mounted in the environmental chamber of an Instron machine. Films were drawn at or slightly above the glass transition temperature. After drawing, the sample was cooled rapidly to ambient temperature while still in the grips. The average thickness (l) of each specimen was determined from the measured density after the barrier measurement was completed.[24] A density gradient column was constructed from a solution of calcium nitrate/water in accordance with ASTM-D 1505 Method B. The column was calibrated with glass floats of known densities. A small piece ($\sim$ 50 mm^2) of film was placed in the column and allowed to equilibrate for 30 min before the measurement was taken.

Dynamic mechanical measurements were carried out in a DMTA Mk II unit from Polymer Laboratories (Amherst, MA) operating in the tensile mode. To examine the subambient γ-relaxation region, measurements were made at a frequency of 1 Hz with a heating rate of 3°C min^{-1}. Measurements in the glass transition region were performed at a frequency of 0.1 Hz and a heating rate of 1°C min^{-1}.

Films for oxygen flux measurements were conditioned as described previously,[24] to obtain the non-steady-state oxygen flux, $J(t)$, from which the permeability (P), diffusivity (D), and solubility coefficient (S) were determined. Oxygen flux was measured with a MOCON OXTRAN® 2/20 at 23°C, 0% relative humidity, and 1 atm pressure.

The conformational composition of each film was determined by photoacoustic Fourier transform infrared (FTIR) spectroscopy. Infrared spectra were collected at ambient temperature with a Nicolet 870 FTIR spectrometer in the photoacoustic mode by using an MTEC Model 200 photoacoustic cell. Samples (10 mm in diameter) were cut from each film after barrier measurement. All infrared specimens were dried overnight under vacuum at ambient temperature. For each sample, 256 scans were collected with a resolution of 4 cm^{-1} and mirror velocity of 0.158 cm s^{-1}. The 1500- to 1400^{-1}-cm region of the spectrum was deconvoluted into three Gaussian peaks using Origin 4.1 software. The relative amounts of *gauche* and *trans* glycol conformations were obtained from the relative peak heights of the 1477 cm^{-1} (*trans*) and 1456 cm^{-1} (*gauche*) bands as described previously.[25] The *trans* fraction is reported as the ratio of the normalized 1477 cm^{-1} peak height to the normalized 1477 cm^{-1} peak height for 100% *trans* conformers.

RESULTS AND DISDUSSION

Synthesis and structural characterization

Polymerization of the PET-*co*-BEHQ copolymers proceeds through a two-step process. The first step is an ester interchange catalyzed by $Mn(OAc)_2$ during which DMT reacts with excess EG to form bis(2-hydroxyethyl)terephthalate (BHET) by the removal of methanol. After this phase is complete, polyphosphoric acid (PPA) is added to quench the manganese catalyst. BEHQ is added with Sb_2O_3, which catalyzes the second phase of the polymerization in which the excess EG is distilled and high molecular weight polymer is formed. Despite the later addition of BEHQ, EG is removed preferentially under these conditions, owing to its lower boiling point. The polymerization of the homopolymer, p(BEHQ-T), proceeds through a one-step ester interchange reaction. Due to the low volatility of the starting materials (DMT and BEHQ), the preparation of high molecular weight polymer depends solely on the removal of methanol through the reaction of end groups. Thus, the monomers were combined at a 1 : 1 molar ratio and the mixture was stirred in the melt for 3 h prior to the application of vacuum.

PET-*co*-BEHQ copolymers were prepared at 5, 10, 15, and 20%. The PET-*co*-BEHQ-Me_4 and PET-*co*-BEHQ-$(OMe)_2$ copolymers were both prepared at a composition of 10%, to compare the effect of substituents on the copolymer properties. The amount of BEHQ incorporated into the PET-*co*-BEHQ copolymers was deter-

TABLE I
Characterization of PET-*co*-BEHQ Polymers

Sample	BEHQ charged (mol %)	BEHQ incorporated[a] (mol %)	IV[b] (dL/g)	10^3 M_n[c] (g/mol)
PET	0	0	0.612	19
PET-*co*-6% BEHQ	6	6	0.647	21
PET-*co*-8.5% BEHQ	10	8.5	0.636	20
PET-*co*-12.5% BEHQ	15	12.5	0.712	23
PET-*co*-16.5% BEHQ	20	16.5	0.654	21
p(BEHQ-T)	100	100	0.648	21
PET-*co*-8% BEHQ-Me_4	10	8.0	0.583	18
PET-*co*-9.5% BEHQ-OMe_2	10	9.5	0.632	20

[a] Determined by ^{1}H-NMR.
[b] Determined in dichloroacetic acid.
[c] Determined by M_n = 34,860 (IV)$^{1.205}$.

mined by using ^{1}H-NMR by comparing the integral of the peak from the hydroquinone protons (6.98, 6.70, or 2.19 ppm) to the integral of the peak resulting from the terephthalate protons (8.15 ppm). Between 80 and 100% of the amount of comonomer charged into the copolymerization reaction was incorporated into the copolymers. The lower than expected amount of BEHQ is due to its partial removal during the relatively rapid vacuum distillation of EG. All the polymers have similar intrinsic viscosities. The composition, intrinsic viscosity, and molecular weight, M_n, of the polymers are shown in Table I.

Thermal analysis

The thermal properties of the BEHQ-containing polymers are shown in Table II. As the amount of BEHQ comonomer present in the polymer increases, the glass transition temperature (T_g), crystallization temperature (T_c), melting temperature (T_m), and heat of melting (ΔH_m) of the polymer decrease. The cold crystallization temperature (T_{cc}) decreases as the comonomer content approaches 10% and then increases at higher comonomer content. The same is true for the PET-*co*-BEHQ-$(OMe)_2$ copolymer. The PET-*co*-BEHQ-Me_4 copolymer exhibits slightly different behavior. The T_g and T_{cc} temperatures are both higher than those for PET. At comomoner contents lower than 10%, all the copolymers exhibit both crystallization from the melt and cold crystallization. All the copolymers above 10% showed a significant amount of cold crystallization with no indication of crystallization upon cooling. Therefore, the crystallinity in these polymers is derived solely from cold crystallization. The lack of crystallization upon cooling indicates that the PET-*co*-BEHQ copolymers above 10% crystallize much more slowly than PET. This is supported by the decrease in ΔH_m with increasing comonomer content. These results correlate with the decrease in the structural order of the polymer due to the addition of comonomer. This decreased order in the crystal structure of the polymer is also responsible for the decrease in T_m.

It is important to note that by replacing EG with BEHQ, some of the rigid, polar ester functional groups are removed from the structure of the polymer and replaced by less polar, less rigid ether linkages. This difference in polarity and flexibility is consistent with an increase in segmental motion and the observed decrease in T_g. The homopolymer, p(BEHQ-T), effectively replaces 50% of the ester linkages with ethers. As a result, this polymer has thermal transitions at lower temperatures than the PET-*co*-BEHQ copolymers. The structural regularity of this polymer results in crystallization upon cooling, in contrast to the copolymers, which showed only cold crystallization at higher compositions of BEHQ. The only thermal transitions observed during DSC analysis resulted from melting and crystallization. There was no evidence of any other transitions that would suggest

TABLE II
Thermal Transitions of PET-*co*-BEHQ Polymers

Sample	T_g (°C)	T_m (°C)	T_c (°C)	T_{cc} (°C)	ΔH_m (J/g)	ΔC_p [J/(g°C)]
PET	76	246	177	157	34.2	0.22
PET-*co*-6% BEHQ	75	238	170	150	29.9	0.28
PET-*co*-8.5% BEHQ	74	231	162	155	25.7	0.30
PET-*co*-12.5% BEHQ	72	218	N/A	164	17.1	0.33
PET-*co*-16.5% BEHQ	70	208	N/A	169	4.12	0.27
p(BEHQ-T)	64	199	126	115	38.1	0.28
PET-*co*-8% BEHQ-Me_4	79	233	170	163	24.2	0.34
PET-*co*-9.5% BEHQ-OMe_2	72	229	137	139	22.2	0.32

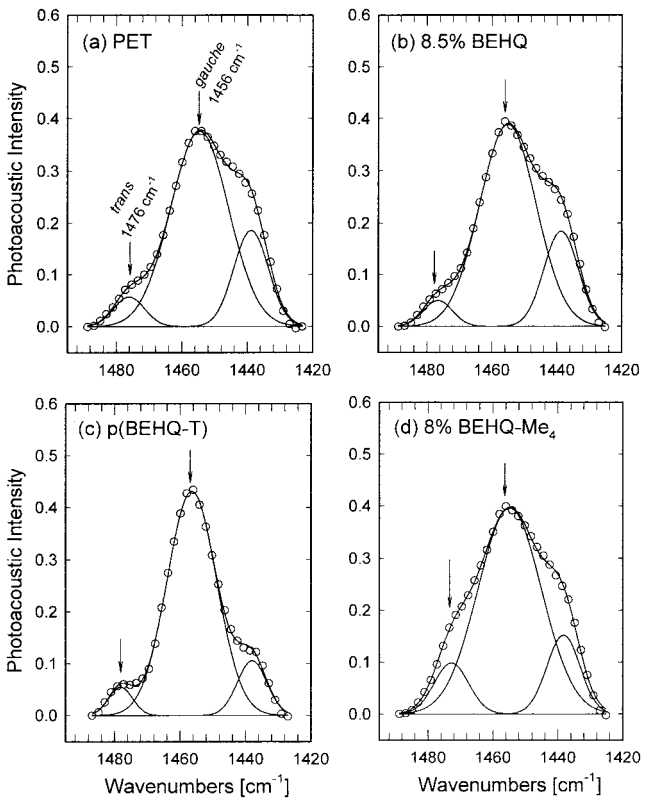

Figure 3 The 1500- to 1400-cm^{-1} Region of the infrared spectrum deconvoluted into three Gaussian peaks: (a) PET; (b) PET-*co*-8.5% BEHQ; (c) p(BEHQ-T); (d) PET-*co*-8% BEHQ-Me$_4$.

that there was a more ordered phase present as a result of enhanced interchain interactions between the electron-poor and electron-rich arenes in the polymer chain. The fact that the polymers are colorless suggests that there are no significant charge–transfer interactions.

Conformer characterization

Specific bands assigned to *trans* and *gauche* conformers of the PET glycol appear in three regions of the spectrum:[26–28] 1500–1400, 1400–1300, and 1000–800 cm^{-1} (Fig. 3). The glycol regions in the spectrum of the p(BEHQ-T) film closely resemble those of PET, and band assignments for p(BEHQ-T) were made accordingly. The *trans* band at 1477 cm^{-1} and the *gauche* band at 1457 cm^{-1} were used for quantitative determination of conformer populations.

Spectra were normalized to the carbonyl band at about 1730 cm^{-1},[29] and the 1500- to 1400-cm^{-1} region was deconvoluted into three Gaussian peaks. The relative amounts of *gauche* and *trans* conformers were obtained from the peak heights by using the published calibration curve for PET.[29] The *trans* fraction (f_t) is reported as the ratio of the normalized height of the peak at 1477 cm^{-1} to the normalized peak height for 100% *trans* conformers (Table III). The *trans* fraction is approximately 0.08–0.09 for all the amorphous films except the copolymers with 8 mol % tetramethyl-substituted BEHQ and 9.5 mol % dimethoxy-substituted BEHQ. These have about double the *trans* fraction of the unsubstituted analog. The significant reduction in *gauche* glycol conformers is attributed to steric hindrance from the methyl and methoxy groups.

Orientation transforms some *gauche* glycol conformations to *trans* conformations, as shown in Table IV. For most of the polymers, a draw ratio of slightly more than 4 increases the *trans* fraction from 0.8–0.9 to 0.27–0.30. The exception was p(BEHQ-T). A smaller increase in *trans* fraction from 0.9 to only 0.13 is consistent with smaller changes observed in specific volume and oxygen solubility for oriented p(BEHQ-T) compared to the copolymers.

Oxygen barrier

As the amount of BEHQ comonomer in the polymer was increased, the oxygen permeability of the amorphous polymer decreased (Table III). The decrease in permeability (P) is due primarily to the decrease in solubility (S). The contribution of S to the permeability of p(BEHQ-T) is slightly offset by a small increase in diffusivity (D).

TABLE III
Oxygen Barrier Properties of Unoriented PET-*co*-BEHQ Polymers[a]

Sample	Density (g/cm^3)	T_g[b] (°C)	f_t[c]	P [cc(STP)cm/ m^2/atm/day]	D (10^{-13} m^2/s)	S [cc(STP)/cm^3/atm]
PET	1.3370 ± 0.0004	81	0.09	0.393 ± 0.004	5.0 ± 0.1	0.092 ± 0.002
PET-*co*-6% BEHQ	1.3348 ± 0.0001	79	0.08	0.379 ± 0.005	5.1 ± 0.2	0.086 ± 0.002
PET-*co*-8.5% BEHQ	1.3339 ± 0.0007	78	0.09	0.357 ± 0.003	5.1 ± 0.2	0.080 ± 0.000
PET-*co*-12.5% BEHQ	1.3332 ± 0.0001	76	0.08	0.340 ± 0.003	5.0 ± 0.1	0.079 ± 0.002
PET-*co*-16.5% BEHQ	1.3319 ± 0.0004	74	0.08	0.329 ± 0.001	5.1 ± 0.2	0.075 ± 0.003
p(BEHQ-T)	1.3083 ± 0.0004	63	0.09	0.289 ± 0.003	5.7 ± 0.2	0.059 ± 0.001
PET-*co*-8% BEHQ-Me$_4$	1.3214 ± 0.0002	83	0.16	0.355 ± 0.001	4.7 ± 0.4	0.088 ± 0.007
PET-*co*-9.5% BEHQ-OMe$_2$	1.3335 ± 0.0003	75	0.20	0.340 ± 0.002	4.7 ± 0.1	0.084 ± 0.003

[a] 1 atm, 0% relative humidity, 23°C.
[b] Determined by DMTA at 0.1 Hz.
[c] *trans* fraction.

TABLE IV
Oxygen Barrier Properties of Oriented PET-*co*-BEHQ Polymers[a]

Sample	λ	Orientation temperature	Density (g/cm^3)	f_t^b	P [cc(STP)cm/ m^2/atm/day]	D (10^{-13} m^2/s)	S [cc(STP)/ cm^3/atm]	Extrapolated ν_0 (cm^3 g^{-1})
PET	4.0	$T_g-10°C$	1.3537 ± 0.0010	0.27	0.187	3.6	0.060	0.721
PET-*co*-6% BEHQ	4.1	$T_g-10°C$	1.3515 ± 0.0007	0.30	0.183	3.9	0.055	0.725
	4.1	T_g	1.3515 ± 0.0007	0.30	0.201	3.8	0.061	
PET-*co*-12.5% BEHQ	4.4	$T_g-10°C$	1.3421 ± 0.0005	0.27	0.258	4.6	0.065	0.728
	4.5	T_g	1.3391 ± 0.0005	0.23	0.271	4.7	0.066	
PET-*co*-16.5% BEHQ	4.4	T_g	1.3461 ± 0.0015	0.39	0.226	4.8	0.054	0.729
	4.6	$T_g+10°C$	1.3465 ± 0.0010	0.37	0.229	4.8	0.055	
p(BEHQ-T)	4.0	T_g	1.3140 ± 0.0020	0.13	0.166	4.1	0.047	0.748
	4.0	$T_g+10°C$	1.3148 ± 0.0008	0.14	0.168	4.3	0.045	
PET-*co*-8% BEHQ-Me_4	4.0	$T_g-10°C$	1.3309 ± 0.0008	0.36	0.224	3.8	0.069	0.732
	4.4	T_g	1.3306 ± 0.0009	0.34	0.241	4.0	0.070	
PET-*co*-9.5% BEHQ-OMe_2	4.4	$T_g-10°C$	1.3435 ± 0.0008	0.31	0.206	3.6	0.066	0.726
	4.6	T_g	1.3416 ± 0.0009	0.29	0.201	3.4	0.068	

[a] 1 atm, 0% relative humidity, 23°C.
[b] *trans* fraction.

The change in solubility with copolymer composition parallels the change in T_g as measured by DMTA at 0.1 Hz (Table 3). The correlation between S and T_g is consistent with free-volume concepts of gas solubility in glassy polymers. In simplified terms, the permeation of small gas molecules through a glassy polymer is viewed as proceeding by jump motion whereby a permeant molecule spends most of the time in free-volume cavities and occasionally jumps into a neighboring cavity. The jump motion proceeds by formation of a channel between two neighboring holes. Thus, gas permeation depends on the number and size of cavities in the polymer matrix and the frequency of channel formation. In a glassy polymer, gas transport occurs under nonequilibrium conditions wherein the polymer possesses more free volume than it would at equilibrium. Sorption is interpreted as the process of filling the holes of excess free volume. The excess-hole free volume in the nonequilibrium glassy polymer is larger than the equilibrium free volume by an amount that depends on the temperature relative to T_g and on the difference between the equilibrium and glassy specific thermal expansivities.[11] For PET and many copolymers based on PET, this interpretation of solubility leads to the solid line correlation in Figure 4.[10] Correspondence between the linear correlation and S of BEHQ homopolymer and copolymers is consistent with the free volume concept of oxygen solubility.

Less excess-hole free volume translates as higher density for glassy polymers of similar chemical structure (i.e., polymers with the same core density defined as the density of the glassy polymer with zero solubility). The

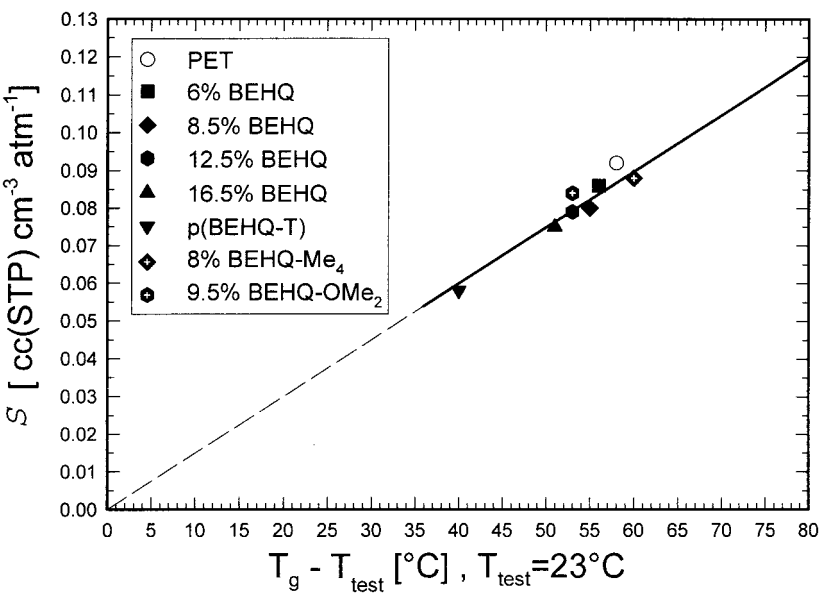

Figure 4 Relationship between solubility and the difference between T_g measured by DMTA at 0.1 Hz and test temperature.

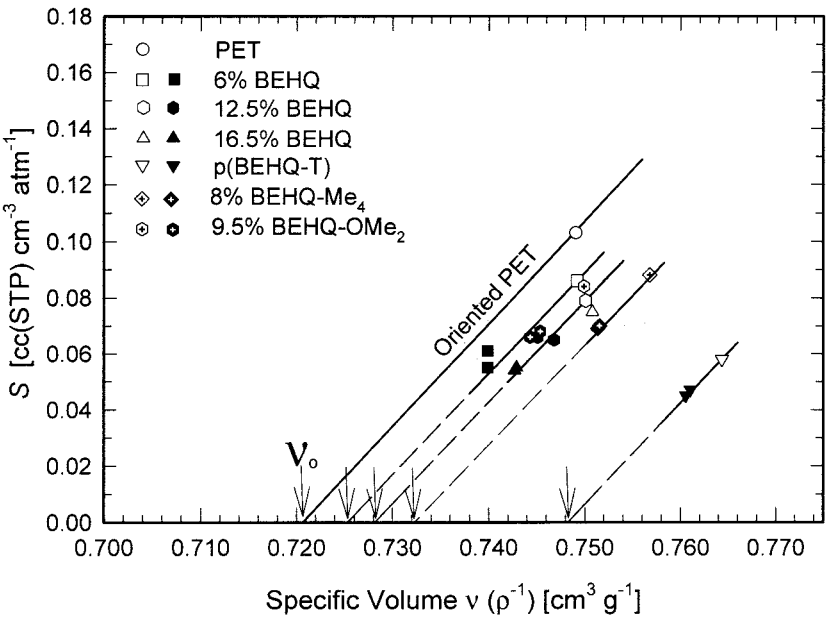

Figure 5 Relationship between solubility and specific volume ($\nu = \rho^{-1}$). Filled symbols are unoriented amorphous polymers; open symbols are cold-drawn polymers.

solid line in Figure 5 with a slope of 3.6 cc(STP) g cm^{-6} atm^{-1} and extrapolated zero-solubility specific volume ν_0 of 0.721 cm^{-3} g describes the relationship between solubility and specific volume of PET. It comes from previous publications in which a single linear relationship between oxygen solubility and amorphous-specific volume described many amorphous PET-based copolymers, densified amorphous PET obtained by cold-drawing, and dedensified PET obtained by crystallization.[10,11,24,29] The BEHQ copolymers systematically deviated from the PET line. The shift could indicate a change in slope of the S versus ν relationship, and/or an increase in ν_0. The slope is related to the density of sorbed oxygen, and a slope change would indicate a fundamental difference between PET and p(BEHQ-T) in the nature of the free volume.

To obtain additional points that would define the relationship between S and ν of the BEHQ, copolymers and p(BEHQ-T) were densified by cold-drawing. The results indicate that the slope did not change. Replacing the ester linkage with an ether linkage does not affect the fundamental characteristics of the excess-hole free volume. The extrapolated values of ν_0 are entered in Table IV. In contrast to the constancy in the slope of the S versus ν relationship, a large increase in extrapolated ν_0 resulted from incorporating BEHQ (Table IV). Evidently, the specific volume at zero solubility is a characteristic of the polymer chemical structure.

Diffusivity derives from jumps of the gas molecule between free volume holes and depends on conformational changes and segmental motions of the polymer chain. In a glassy polymer, it seems reasonable that these thermal rearrangements would manifest themselves as sub-T_g relaxation processes. Indeed, a relationship between diffusivity and the γ-relaxation, particularly the relaxation component associated with *gauche* conformations of the glycol, was demonstrated previously for PET and copolymers based on PET.[10,11]

Relaxation behavior of the BEHQ polymers is reported as log E'' in Figure 6. Relative to PET, the higher diffusivity of p(BEHQ-T) is not consistent with the lower γ-relaxation intensity measured as the area under the E'' curve. However, BEHQ also affects the shape of the relaxation. The complexity of the γ-relaxation of PET has led to identification of a lower temperature component with *gauche* conformations of the glycol and a higher temperature component with *trans* conformations of the glycol.[30–32] Motion of *gauche* conformers appears to be more effective for enabling the jump motion of penetrant molecules between free-volume holes. The shift to lower apparent relaxation temperature with increasing BEHQ content suggests an increase in the *gauche* relaxation component relative to the *trans* component. Greater mobility of *gauche* glycol conformers in which an ether linkage replaces an ester linkage could account for higher diffusivity of p(BEHQ-T).

CONCLUSION

Incorporation of BEHQ, tetramethyl BEHQ, and dimethoxy BEHQ into PET improves the O_2 barrier properties of the resulting copolymers. This increase is largely due to the decrease in the solubility of O_2 in the polymers. Solubility depended on the glass transition of the copolymer in accordance with free-volume concepts of gas permeability. With a 26% improvement over PET, the p(BEHQ-T) homopolymer shows a higher barrier than the copolymers studied. Orienting

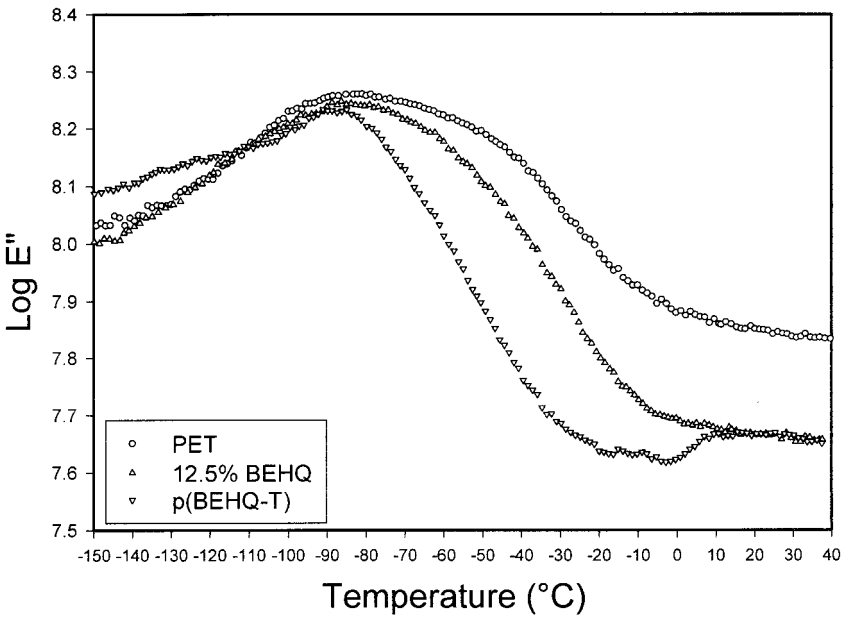

Figure 6 Temperature dependence of log E″ in the γ-relaxation region.

amorphous films of p(BEHQ-T) results in further improvement of the oxygen barrier properties.

We thank Joseph Campbell for help with the preparation of the PET-*co*-BEHQ copolymers. We also thank KoSa for support of this research, along with the UNCF-Merck Science Initiative and the GEM Consortium for awards to G.S.A.

References

1. Modern Plastics World Encyclopedia, Vol. 12; Modern Plastics; 1999; pp. A196–A201.
2. Freeman, B. D.; Hill, A. J. in Structure and Properties of Glassy Polymers; Tant, M. R.; Hill, A. J., Eds.; ACS Symposium Series 710; American Chemical Society: Washington, DC, 1998; pp. 306–325.
3. Cahill, P. J. World Pat. 12,244, 1998.
4. Shimizu, S.; Nagano, M.; Ishizeki, T.; Momose, Y. Eur. Pat. 180,191, A1, 1986.
5. Socci, E. P.; Akkapeddi, M. K.; Worley, D. C. Annual Technical Conference; Society of Plastics Engineers, 2001; pp. 1721–1725.
6. Lange, J.; Stenroos, E.; Johansson, M.; Malmstrom, E. Polymer 2001, 17, 7403.
7. Adamantiadi, A.; Badeka, A.; Kontominas, M. G. Food Addit Contam 2001, 11, 1046.
8. Flodberg, G.; Hojvall, L.; Hedenqvist, M. S.; Sadiku, E. R.; Gedde, U. W. Polym Mater 2001, 2, 157.
9. Po, R.; Occhiello, E.; Giannotta, G.; Pelosini, L.; Abis, L. Polym Adv Technol 1996, 5, 365.
10. Polyakova, A.; Connor, D. M.; Collard, D. M.; Schiraldi, D. A.; Hiltner, A., Baer, E. J Polym Sci, Part B: Polym Phys 2001, 16, 1900.
11. Polyakova, A.; Liu, R. Y. F.; Schiraldi, D. A.; Hiltner, A.; Baer, E. J Polym Sci, Part B: Polym Phys 2001, 16, 1889.
12. Silvis, H. C. Trends Polym Sci 1997, 3, 75.
13. Jackson, W. J. Mol Cryst Liq Cryst 1989, 169, 23.
14. (a) Harkness, B. R.; Wanatabe, J. Macromolecules 1991, 24, 6759; (b) Sone, M.; Harkness, B. R.; Wanatabe, J.; Yamashita, T.; Torii, T.; Horie, K. Polym J 1993, 9, 997; (c) Sone, M.; Wada, T.; Harkness, B. R.; Wanatabe, J.; Takahashi, H.; Huang, H. W.; Yamashita, T.; Horie, K. Macromolecules 1998, 31, 8865.
15. Khan, A. U.; Kearns, D. R. J Chem Phys 1968, 7, 3272.
16. Birks, J. B.; Pantos, E.; Hamilton, T. D. S. Chem Phys Lett 1973, 6, 544.
17. Khalil, G. E.; Kasha, M. Photochem Photobiol 1978, 28, 435.
18. Tsubomura, H.; Mulliken, R. S. J Chem Phys 1960, 82, 5966.
19. Scurlock, R. D.; Ogilby, P. R. J Phys Chem 1989, 93, 5493.
20. Capitani, D.; Segra, A. L.; Barsacchi, M.; Pentimalli, M. Eur Polym J 1999, 35, 681. Capitani, D.; Clericuzio, M.; Fiordiponti, P.; Lillo, F.; Segre, A. L. Eur Polym J 1993, 11, 1451.
21. Yasunori, H.; Fumito, S.; Takahiro, S. 7188523, 1995. Yasunori, H.; Yukihiro, N.; Shinji, O.; Kiyoshi, S. Jap. Pat. 7,188,531, 1995; Yasunori, H.; Fumito, S.; Takahiro, S. 7188522, 1995. Yasunori, H.; Fumito, S.; Takahiro, S. Jap. Pat. 7,188,530, 1995; Yasunori, H.; Yukihiro, N.; Shinji, O.; Kiyoshi, S. Jap. Pat. 7,188,525, 1995; Yasunori, H.; Yukihiro, N.; Shinji, O.; Kiyoshi, S. Jap. Pat. 7,188,524, 1995; Fumito, S.; Yasunori, H. Jap. Pat. 6,211,973, 1994.
22. Sun, Y. M.; Wang, C. S. J Polym Sci, Part A: Polym Chem 1996, 34, 1783.
23. Qureshi, N.; Stepanov, E. V.; Schiraldi, D.; Hiltner, A.; Baer, E. J Polym Sci, Part B: Polym Phys 2000, 38, 1679.
24. Sekelik, D. J.; Stepanov, S. V.; Nazanrenko, S.; Schiraldi, D.; Hiltner, A.; Baer, E. J Polym Sci, Part B: Polym Phys 1999, 37, 847.
25. Miyake, A. J Polym Sci 1959, 38, 479.
26. Miyake, A. J Polym Sci 1959, 38, 497.
27. Lin, S.-B.; Koenig, J. L. J Polym Sci, Part B: Polym Phys Ed 1982, 20, 2277.
28. Cole, K. C.; Daly, H. B.; Sanschagrin, B.; Nguyen, K. T.; Ajji, A. Polymer 1999, 40, 3505.
29. Liu, R. Y. F.; Schiraldi, D. A.; Hiltner, A.; Baer, E. J Polym Sci, Part B: Polym Phys 2002, 40, 3505.
30. Uralil, F.; Sederel, W.; Anderson, J. M.; Hiltner, A. Polymer 1979, 20, 51.
31. Illers, K. H.; Breuer, H. J. Colloid Sci 1963, 18, 1.
32. Armeniades, C. D.; Baer, E. J Polym Sci, Part A-2: Polym Phys 1971, 9, 1345.